Application of the second order generalized integrator in digital control systems

KAMIL MOŻDŻYŃSKI[1], KRZYSZTOF RAFAŁ[2], MAŁGORZATA BOBROWSKA-RAFAŁ[1]

[1]*Faculty of Electrical Engineering, Warsaw University of Technology*
Koszykowa 75, 00-662 Warszawa
e-mail: {mozdzynk/bobrowsm}@ee.pw.edu.pl

[2]*Faculty of Mechanical and Aerospace Engineering, Warsaw University of Technology*
Koszykowa 75, 00-662 Warszawa
e-mail: krafal@itc.pw.edu.pl

Abstract: The paper describes second order generalized integrator (sogi) which is specialized in band-pass filtering and orthogonalization of periodic signals. Modifications of the structure and the influence of parameters on the system performance is described. The article highlights the particular importance of model discretization method in the practical implementation, as well as reviews estimation methods of the: amplitude, frequency, offset and phase angle of the periodic signal. Examples of simulation and experimental results are presented.

Key words: second order generalized integrator, digital implementation, DSP

1. Introduction

Development of control methods for power electronics converters requires new solutions for the monitoring and regulation of periodic signals. The main issue in this field is to provide an accurate estimation of the parameters of selected components of the signal (amplitude, frequency, offset and phase angle). Currently the most commonly used structure for this purpose is Phase Locked Loop (PLL) [14]. Another issue is the practical implementation of regulators which are developed in continuous domain. In discrete domain it is desired that executable code requires minimal computational effort from the control unit. It is also important to change the structure parameters without additional calculations. This applies to the corresponding discretization of the continuous model, where the most frequently used method is based on transformation from the continuous to discrete transfer function. These transformations require long calculation and occupy additional memory space in the control unit.

Article describes an estimation method of periodic signals parameters based on the Second Order Generalized Integrator SOGI. By additional structure extensions and choice of the

appropriate parameter values a very good dynamics and resistance to interference in signal processing can be achieved.

Functions based on SOGI allow:

- band-pass, low-pass and band-stop filtering;
- estimation of harmonic signal parameters: amplitude, frequency, offset and phase angle [1, 9-11];
- generation of a tracking reference waveforms or regulated phase shifted reference waveforms [16];
- control and compensation of harmonic components as a part of the Proportional-Resonant (PR) controller [2].

The key of the application (for the above features) is the continuous model discretization, which is presented in this paper. The article proposes the rarely used and not yet defined method for structural discretization [15]. It consists of substituting continuous integrator from block diagram by chosen discrete integrator block. Then determines the type of each node and determines the set of equations reflect the variables flow in discrete model. This solution appears to meet the demands of implementation and simplifies it, eliminating the continuous to discrete conversion of the transfer function by the control unit.

In previous works a detailed applications of the SOGI as a current controller for grid-connected converters were defined: single-phase grid connected inverters [4-7], three-phase grid connected inverters [8], active filters [12], stator current harmonic control for doubly fed induction generator [13]. In most of these works the problem of discretization is described [3], however, the optimal form of practical implementation has not been finally defined.

The paper presents an analysis of second order generalized integrator and additional structure extensions that allow estimation of the parameters of a periodic signal. In subsequent chapters specific impact of discretization on the practical implementation was discussed. Furthermore, the examples of application were described.

2. Second order generalized integrator

2.1. Continuous domain model

Structure of SOGI is presented in Figure 1. This model is described by the Equations (1) and (2). SOGI properties result from the conjugated poles $\pm j\omega_0$ located on the border of stability (MRI). Bode Diagrams of SOGI (Fig. 2) shows an infinite gain for the resonant frequency. Confirmation of that fact is the time response for a periodic signal with frequency equal to resonant frequency presented in Figure 3.
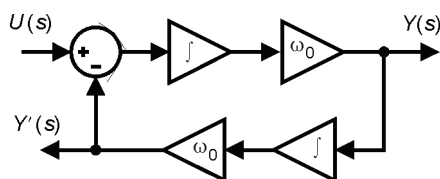

Fig. 1. SOGI in continuous time-domain

$$\frac{Y(s)}{U(s)} = \frac{\omega_0 s}{s^2 + \omega_0^2},$$

(1)

$$\frac{Y'(s)}{U(s)} = \frac{\omega_0^2}{s^2 + \omega_0^2}.$$
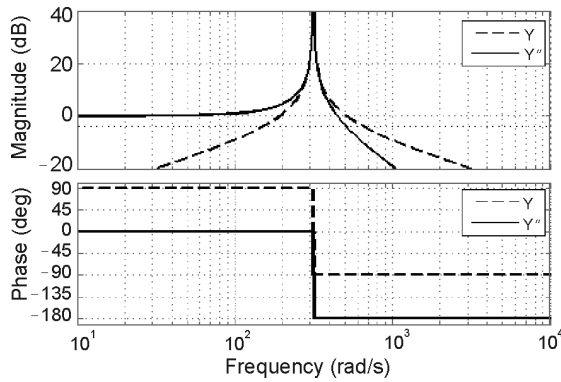
(2)

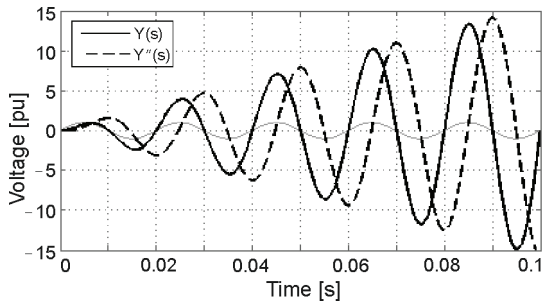Fig. 2. Bode diagram of SOGI of the continuous time-domain

Fig. 3. Step response of SOGI

2.2. Feedback loop

The presence of resonance in SOGI structure causes a continuous growth of the output signals amplitude. When signal is processed by SOGI in a digital system there is a problem with the overflow of dedicated variables. To prevent this, structure is closed with the feedback loop from the output signal $Y(s)$ as shown in Figure 4.
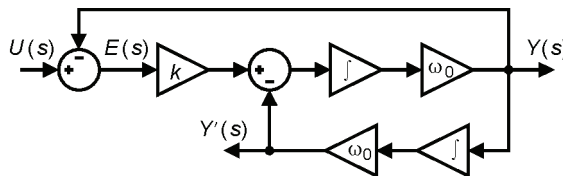

Fig. 4. SOGI-OSG in continuous time-domain

As a result, the transfer function takes the form of Equation (3) for direct output, and (4) for orthogonal output.

$$\frac{Y(s)}{U(s)} = \frac{k\omega_0 s}{s^2 + k\omega_0 s + \omega_0^2},$$ (3)

$$\frac{Y'(s)}{U(s)} = \frac{k\omega_0^2}{s^2 + k\omega_0 s + \omega_0^2}.$$ (4)

Bode Diagrams exhibit nature of the band-pass compatible output $Y(s)$ (Fig. 5) and the low-pass nature of the output $Y'(s)$, which is phase-shifted (Fig. 6). SOGI structure with feedback loop extension is defined as Orthogonal Signal Generator SOGI-OSG. The parameter k amplifying error signal $E(s)$ affects the filter bandwidth and the transient response. The choice of the parameter k requires a compromise between good signal filtering and system response dynamics (Fig. 7).
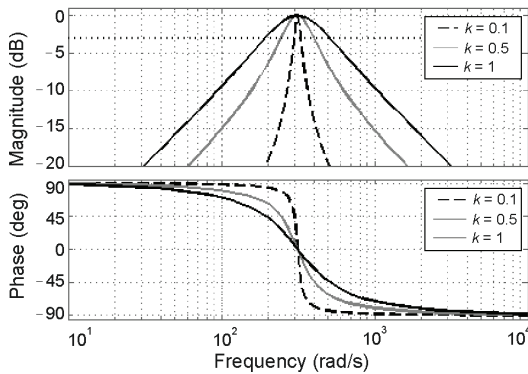

Fig. 5. Bode Diagram of compatible output $Y(s)$ of SOGI-OSG of the continuous time-domain
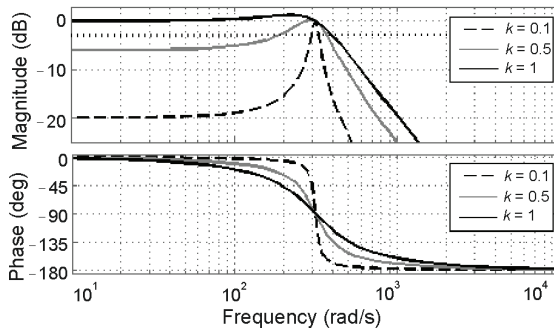

Fig. 6. Bode Diagram of orthogonal output $Y'(s)$ of SOGI-OSG of the continuous time-domain

One should also pay attention to the signal $E(s)$ which is the difference between input $U(s)$ and output $Y(s)$ described by following transfer function:

$$\frac{E(s)}{U(s)} = \frac{s^2 + \omega_0^2}{s^2 + k\omega_0 s + \omega_0^2}.$$ (5)

As a result it represents the notch filter (Fig. 8). This feature is useful in signal offset estimation, where it is assured that the signal contains one fundamental harmonic and DC component (6). Offset estimation is shown in the Equations (7)-(11).
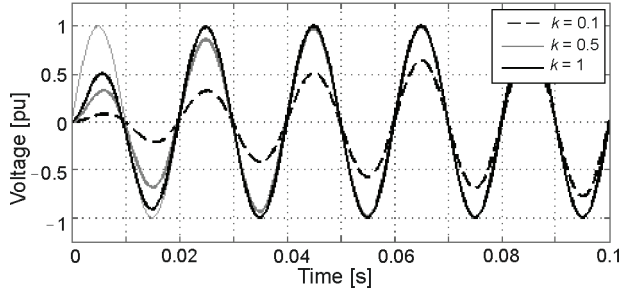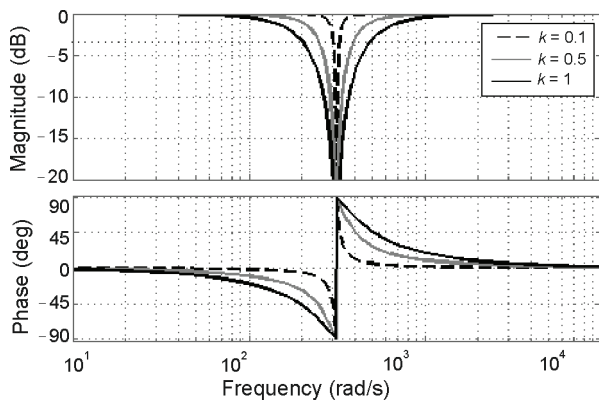
Fig. 7. Step response of SOGI-OSG

Fig. 8. Bode Diagram of orthogonal output $Y'(s)$ of SOGI-OSG of the continuous time-domain

$$u(t) = A_0 \cdot 1(t) + A_1 \sin(\omega_0 t), \tag{6}$$

$$U(s) = \frac{A_0}{s} + \frac{A_1 \omega_0}{s^2 + \omega_0^2} = \frac{A_0\left(s + \frac{A_1}{A_0}\omega_0 + \frac{\omega_0^2}{s}\right)}{s^2 + \omega_0^2}, \tag{7}$$

$$E(s) = \frac{s^2 + \omega_0^2}{s^2 + k\omega_0 s + \omega_0^2} \cdot \frac{A_0\left(s + \frac{A_1}{A_0}\omega_0 + \frac{\omega_0^2}{s}\right)}{s^2 + \omega_0^2} = \frac{A_0\left(s^2 + \frac{A_1}{A_0}\omega_0 s + \omega_0^2\right)}{s\left(s^2 + k\omega_0 s + \omega_0^2\right)}, \tag{8}$$

$$k = \frac{A_1}{A_0}, \tag{9}$$

$$E(s) = \frac{A_0}{s}, \tag{10}$$

$$e(t) = A_0 \cdot 1(t). \tag{11}$$

2.3. Frequency locked loop

SOGI-OSG described in previous section has one major drawback. When resonant frequency is different than input signal frequency or there are frequency variations SOGI output

loses tracking accuracy. As a result SOGI-OSG with constant resonant frequency is used only where the designer is confident about the stability of the processed signal frequency and knows its exact value.

Another extension of SOGI structure, called Frequency Locked Loop FLL, is presented in Figure 9.
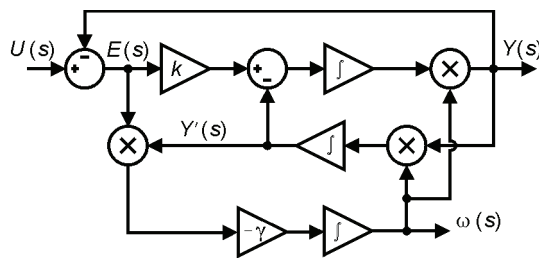

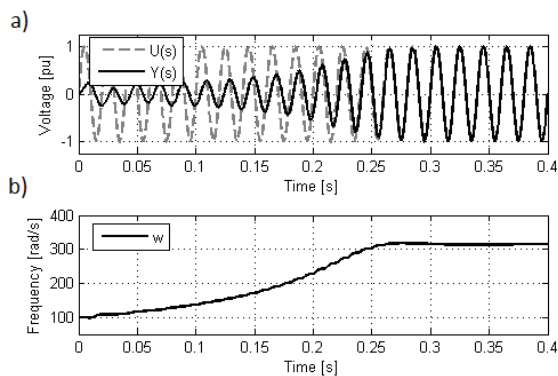Fig. 9. SOGI-FLL in continuous time-domain

Fig. 10. SOGI-FLL step response a) direct output, b) frequency estimated value

Difference between input signal and direct output is multiplied by orthogonal output. This result is then amplified by a factor -γ and subjected to an operation of integration. The ultimate result of these operations is the estimated value of input signal frequency. However the SOGI system, which becomes non-stationary, as a parameter of the resonance frequency, must be continuously updated. This includes practical applications, where continuous to discrete transformation is used. Calculation of the coefficients in a real-time requires their re-transmission in discrete transfer function. Solution to this problem is given in Section 3.2. Example execution of frequency estimation, is shown in Figure 10. SOGI-FLL has one significant disadvantage: when the input signal contains a DC component, the system will be unstable. To prevent this, input signal should be high-pass filtered.

3. Discretization of continuous domain SOGI

Methods for discretization of continuous systems such as: tables of continuous and discrete transfer function, continuous operators, state space equations, are based on the conversion of

continuous transfer function or matrix with defined parameters. This is not a problem, when the system is stationary. Discrete form of the system is determined only once, while for the rest of the time cyclic calculations are performed on the basis of this one form of equations with static parameters. However, in cases where the system is non-stationary, each calculation of outputs function need an additional parameters conversion, which may takes more computational resources than the calculation of system outputs.

To solve the abovementioned problems the method proposed in the article is structured discretization. It consists of several sequential steps. The first task is to bring the system to a block diagram with the continuous domain integrator blocks. Then replace the integrator to its counterpart in the discrete domain in accordance with the chosen method: Euler, Tustin, etc. The result is a flow diagram of the variables, which is the basis to arrange a set of equations implementing the system. However, before the equations are arranged, it is necessary to determine the key state variables and parameters of the system. At this stage, we can distinguish three types of variables that build the structure of the system, and they are: input/output terminals, parameters and internal data (Fig. 11). Input/output terminals means the variables are supplied to a system or retrieved from it. Internal data are variables used only for internal purposes of the system, and the information about them is not needed outside. For example, it may be storing the value for the next iteration. Parameters are constant values resulting from the structure. Having defined variables and their classification, the equation can be arranged starting at the input terminals and ending at the output terminals.
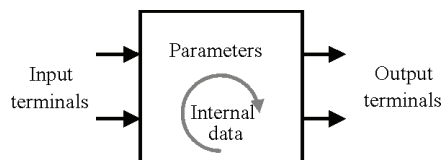

Fig. 11. Pattern structure of discretized object

The most important factors determining the quality of the resulting equations are accurate approximations of the continuous system response, calculation time and the number of variables representing the system. It is desired to achieve the highest accuracy of the approximation in the shortest possible time using the fewest number of variables. In order to verify structured discretization method, tests were conducted using three discrete integrators: Euler backward, Euler forward and bilinear.

3.1. SOGI-OSG discretization example

As to illustrate the structural discretization Euler forward integrator method is used and substituted for its equivalent model in Figure 4. As a result, the following model was obtained:

The next step is to decide how many variables will be necessary to calculate equations and assign them to the appropriate type. At this step the designer has the ability to match the structure of the program code to design needs. For example, it was decided that the information needed outside is signals $y[n]$ and $y'[n]$. In contrast, the value of $e[n]$ is treated as a temporary and classified as an internal data. Just as qualified values $y[n-1]$, $y'[n-1]$ used in the next iteration. This classification is summarized in Table 1.
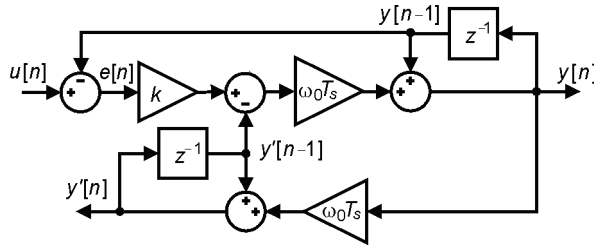
Fig. 12. SOGI-OSG in discrete time-domain with Euler Forward integrators

Table 1. Assignment of variables according to the conceptual model of Figure 10

	Input/output terminal	**Internal data**	**Parameter**
use case	variables which are supplied to a system or retrieved from it	variables used only for internal purposes of the system or storing the value for the next iteration	constant values resulting from the construction of the structure
variables	$u[n]$, $y[n]$, $y'[n]$	$e[n]$, $y[n-1]$, $y'[n-1]$	k, ω_0, T_s

The last step is to put equations on the basis of the flow diagram of variables (Fig. 12). First equation should include input variables and save the results to internal data (12). Only then a set of equations for output variables can be arranged in the correct Sequence (13), (14).

$$e[n] = u[n] - y[n-1], \tag{12}$$

$$y[n] = y[n-1] + (e[n] \cdot k - y'[n-1]) \cdot \omega_0 T_s, \tag{13}$$

$$y'[n] = y'[n-1] + y[n] \cdot \omega_0 T_s. \tag{14}$$

Arrangement of equations also allows the use of multi-step calculation of outputs. Thus, due to the choice of a discrete integrator and flexibility when arranging equations, there can be a huge number of variations. The Table 2 shows three of the possibilities. The maximum error was calculated based on tracking the ideal sine wave by output $y[n]$ which depends on: discretization method, integration period T_s and set of equations.

Table 2. Comparsion of different variants of integration methods, $T_s = 0.00005$ s

	Maximum error [%]	**Number of operations**	**Number of variables**
Euler forward	1.57	7	4
Multi-step euler forward	0.88	15	5
Bilinear	2.25	12	6

Multistep method significantly reduces the approximation error at the expense of the operations amount. In contrast, bilinear method did not produce good results for either of the criteria. The obtained results show the flexibility of the method of structural discretization to achieve the assumed requirements.

3.2. SOGI-FLL discretization example

Developed structure of SOGI-FLL confirms convenience of the structural discretization. Following the scheme in the previous section, after substituting continuous domain integrators with Euler forward discrete integrator in the model of the Figure 9 to give the variable flow diagram (Fig. 13). In this case, the ω_0 parameter becomes the output terminal $\omega[n]$ and is added another parameter γ.
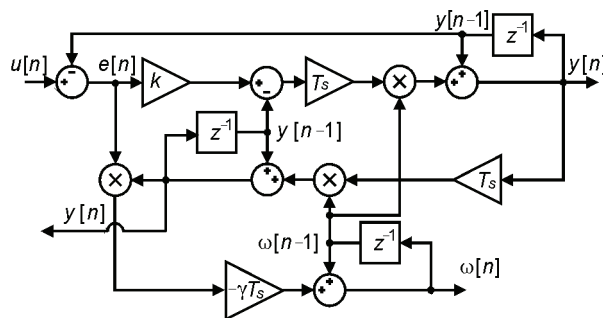

Fig. 13. SOGI-FLL in discrete time-domain with Euler Forward integrators

Then the variable names are assigned to the nodes and arranged in the Eqations (15)-(18).

$$e[n] = u[n] - y[n-1], \tag{15}$$

$$y[n] = y[n-1] + (e[n] \cdot k - y'[n]) \cdot \omega[n-1] \cdot T_s, \tag{16}$$

$$y'[n] = y'[n-1] + y[n] \cdot \omega[n-1] \cdot T_s, \tag{17}$$

$$\omega[n] = \omega[n-1] - \gamma \cdot y'[n] \cdot e[n] \cdot T_s. \tag{18}$$

Athough SOGI become un-stationary system and the necessity of converting discrete transform coefficients was eliminated. It is especially important here to define the initial conditions for the frequency value. This cannot be the zero value because the system will not initiate its operation.

4. Applications

Band-pass filtering properties and orthogonal waveform generation, are crucial for the application of the SOGI. Output signals should contain only the basic harmonic frequency. Achieving properly filtered waveform confirm the accuracy of the implemented algorithms presented in this section.

4.1. Orthogonal Signal Generator and phase angle estimation

Band-pass filtering and orthogonal signal generation gives the possibility to apply it to systems of phase-locked loop (Fig. 14), particularly used to track voltage waveform of power grid voltage. SOGI-OSQ replaces the band-pass filter and trigonometric functions of con-

ventional PLL. An artificial system is created on the basis of the orthogonal and direct outputs, which is then transformed to *dq* Synchronous Rotating Frame. Thus obtained *q* component is given on PI controller. PI output frequency is subjected to integration. The main disadvantage of this structure may be a failure to adapt to fluctuations in the frequency of the input signal. Then SOGI-OSG can be replaced by SOGI-FLL.
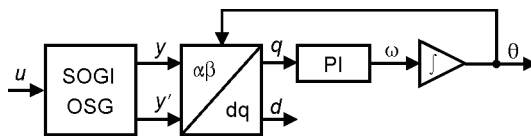

Fig. 14. Phase locked loop based on SOGI-OSG

Simplified method to estimate phase-angle is shown in Figure 15. Reversing output $y[n]$ then using the *arcus tangens* function receives the value of the phase-angle.
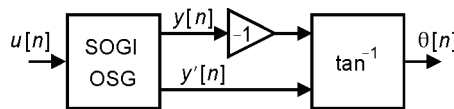

Fig. 15. Phase angle estimation diagram based on SOGI-OSG

4.2. Amplitude estimation

Amplitude of the selected harmonic signal can be estimated on the basis of $y[n]$ and $y'[n]$ outputs in two ways. The first is a conditional detection of the zero crossing for both outputs. When one of the outputs crosses zero, another is at its peak. As a result, the amplitude value is updated four times a period.

$$\begin{cases} A = abs(y[n]) \ \ for \ \ y'[n] = 0 \\ A = abs(y'[n]) \ \ for \ \ y[n] = 0 \end{cases} \tag{19}$$

The second method is to use the properties of sinusoidal functions. If two sine waves of the same amplitude are shifted from each other by 90° of the period, the amplitude is equal to the square root of sum of squares of instantaneous values:

$$A[n] = \sqrt{y[n]^2 + y'[n]^2}. \tag{20}$$

Figure 16 shows the estimated amplitude waveforms, where the impact of pass band width on the accuracy of the estimated amplitude is visualized. In the case of distorted signal $y[n]$ and $y'[n]$ and the wider pass band using the method of (14) shows a greater stability. Both methods are resistant to high frequency noise.

4.3. Frequency estimation

SOGI-FLL structure described in section 2.3 allows tracking of the fundamental frequency of the input signal, simultaneously adjusting the resonance frequency to the estimated value. Dynamics and accuracy depend on the parameters k (band-pass width) and γ. Example results

of frequency estimates progress depending on the parameters were shown in Figure 17 for the k parameter, and Figure 18 for the γ parameter used as an input signal such as shown in Figure 9.

Fig. 16. Amplitude estimation simulation results a) Method (20) b) Method (19)

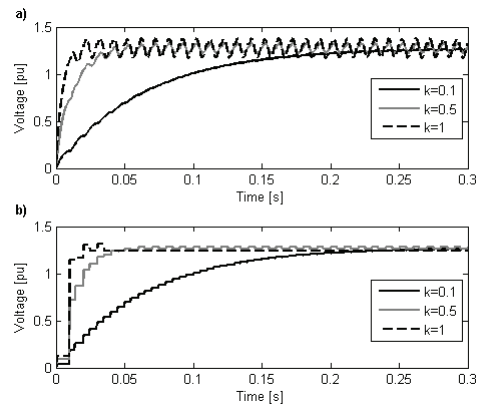Fig. 17. Frequency estimation simulation results for for different values of the γ parameter $k = 0.5$, $\omega = 314.15$
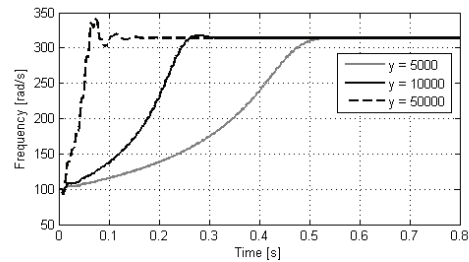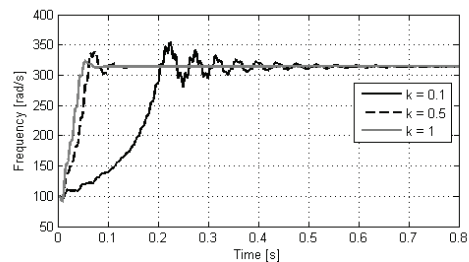

Fig. 18. Frequency estimation simulation results for for different values of the k parameter, $\gamma = 50000$, $\omega = 314.15$

Analysis of the parameter impact has been placed in the Table 3. Wider bandwidth improves the successive values stabilization of the frequency estimation, however, adversely affects the other factors. Parameter γ value selection is a compromise between dynamics and precision of the frequency estimation.

4.4. Normalized sine wave reference signal

The main task of a PLL is the estimation of the phase angle of the signal being tracked. In this way a normalized sine wave reference signal was obtained. As follows from the properties

of SOGI-OSG described in Section 2.2, the direct output tracks the input signal. Thus obtained is a sine wave, can be normalized by dividing by the peak value:

$$S_{ref}[n] = \frac{y[n]}{A[n]}. \tag{21}$$

Table 3. The impact of parameter changes to the SOGI-FLL

Parameter		Dynamic	Filtering	A	f	θ
k	↑	–	–	–	+	–
	↓	+	+	+	–	+
γ	↑	+	0	0	–	0
	↓	–	0	0	+	0

In the case of distorted input signals appropriately narrow bandwidth should be selected by modifying the *k* parameter. In this manner it is possible to replace the entire structure of the PLL by extended SOGI-OSG structure (Fig. 19) which makes possibility to avoid the use of trigonometric functions.
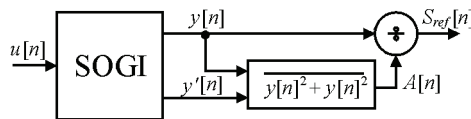

Fig. 19. Reference sine wave signal generator diagram

5. Experimental results

In order to test the feasibility of developed SOGI structure, derived algorithms were implemented on a TMS320F28069 digital signal controller from Texas Instruments [18]. The microcontroller includes two floating-point computational units called CPU and CLA – Control Law Accelerator [19]. There are two cores operating in parallel, at the same 90 MHz clock, where the CPU is the master unit. The input waveforms are assigned directly to the analog to digital converter inputs of the microcontroller with the arbitrary waveform generator. The output waveform was generated by the microcontroller PWM output waveform filtered by RC circuit (hence the apparent phase shift).

Figure 20 shows the waveform of the SOGI-OSG phase-compatible output response to disturbed sinusoidal signal.

Figure 21 shows the waveforms amplitude estimation algorithm, where the input waveform with a frequency of 50 Hz is amplitude modulated. This creates the possibility of using SOGI as an AM demodulator [17]. A similar effect can be achieved for the FM demodulation. This is due to the fact that these quantities are estimated continuously. Figure 22 shows the waveform of reaction SOGI-FLL to step change in frequency and phase of the input signal.

Fig. 20. Red waveform is the distorted input sine wave with offset, blue waveform is signal from phase-compatible SOGI-OSG output
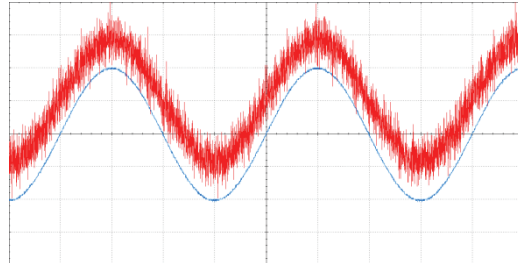

Fig. 21. Blue waveform is the AM modulated 4 Hz sine wave with 50 Hz carried wave, Red waveform is the estimated amplitude
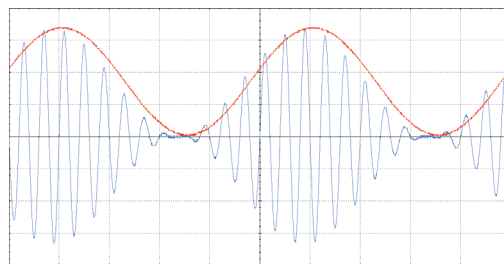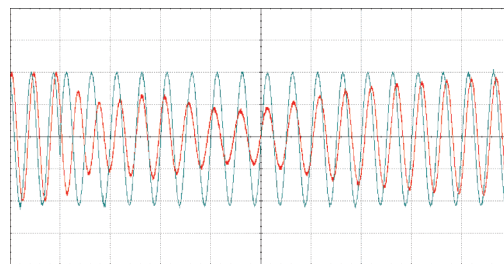

Fig. 22. Green waveform is input signal with frequency step from 80 Hz to 70 Hz, Red waveform is the tracking signal from phase-compatible output

Number of machine cycles needed for the practical implementation of algorithms in Assembler code is given in Table 4. Number of cycles shows the absolutely performance of the algorithm, while the execution time duration depends on embedded system clock frequency. When calculating machine cycles read/write memory operations were included.

Table 4. Summary of execution

	CPU cycles	Variables in memory
SOGI-OSG (Offset)	10 (12)	5 (6)
SOGI-FLL	15	6
Amplitude	21	1
Phase angle	46	1
Reference sine wave	37	6

6. Conclusions

In the paper, the second order generalized integrator with additional extensions was presented. Particular attention was paid to the problem of SOGI discretization. The use of

algorithms based on equations basing on stacked discrete flowchart allows change of the transfer function and eliminating parameters. As a result, achieved the ability to easily modify and adapt the functionality to meet the needs arising from the assignment of the basic parameters of a periodic signal being processed. The main challenge for the designer is to determine the operating conditions and the choice of SOGI extensions parameters, which is a compromise between the response dynamics and the expected accuracy of the estimation.

References

[1] Fedele G., Ferrise A., *Non Adaptive Second-Order Generalized Integrator for Identification of a Biased Sinusoidal Signal.* IEEE Transactions on Automatic Control 57(7): 1838-1842 (2012).

[2] Wang L., Yang T., Zhang D., Lu Z., *A high performance simulation methodology for multilevel grid connected inverters.* Journal of Zhejiang University SCIENCE C 13(7): 544-551 (2012).

[3] Díaz M.J., Bueno E., Mateos R. et al., *FPGA Implementation of Harmonic Detector based on Second Order Generalized Integrators.* 34th Annual Conference of IEEE, Industrial Electronics, pp. 2453-2458 (2008).

[4] Tao H., Duarte J.L., Hendrix M.A.M., *Control of Grid-Interactive Inverters as Used in Small Distributed Generators.* IEEE 42nd IAS Annual Meeting Industry Applications, pp. 1574-1581 (2007).

[5] Sera D., Kerekes T., Lungeanu M. et al., *Low-Cost Digital Implementation of Proportional-Resonant Current Controllers for PV Inverter Applications Using Delta Operator.* 31st Annual Conference of IEEE Industrial Electronics Society, Nov. (2005).

[6] Matas J., Castilla M., de Vicuna L.G. et al., *Virtual Impedance Loop for Droop-Controlled Single-Phase Parallel Inverters Using a Second-Order General-Integrator Scheme.* IEEE Transactions On Power Electronics 25(12): 2993-3002 (2010).

[7] Teodorescu R., Blaabjerg F., Liserre M., Loh P.C., *Proportional-resonant controllers and filters for grid-connected voltage-source converters.* IEEE Proc. Electr. Power Appl. 153(5): 750762 (2006).

[8] Rodriguez P., Luna A., Etxeberria I. et al., *Multiple Second Order Generalized Integrators for Harmonic Synchronization of Power Converter.* IEEE Energy Conversion Congress and Exposition 9: pp. 2239-2246 (2009).

[9] Golestan S., Monfared M., Freijedo F.D., *Design-Oriented Study of Advanced Synchronous Reference Frame Phase-Locked Loops.* IEEE Transaction On Power Electronics 28(2): 765-778 (2013).

[10] Ciobotaru M., Teodorescu R., Blaabjerg F., *A New Single-Phase PLL Structure Based on Second Order Generalized Integrator.* Proc. IEEE Power Electron. Spec. Conf. (PESC'06), Jun., pp. 1-7 (2006).

[11] Reza S., Ciobotaru M., Agelidis V.G., *Tracking of Time-Varying Grid Voltage Using DFT Based Second Order Generalized Integrator Technique.* IEEE Power System Technology (POWERCON), Oct., pp. 1-6 (2012).

[12] Rodríguez A., Girón C., Rizo M. et al., *Comparison of Current Controllers based on Repetitive-Based Control and Second Order Generalized Integrators for Active Power Filters.* 35th Annual Conference of IEEE Industrial Electronics Nov., pp: 3223-3228 (2009).

[13] Liu C., Blaabjerg F., Chen W., Xu D., *Stator Current Harmonic Control With Resonant Controller for Doubly Fed Induction Generator.* IEEE Transaction on Power Electronics 27(7): 3207-3220 (2012).

[14] Golestan S., Monfared M., Freijedo F.D., Guerrero J.M., *Design and Tuning of a Modified Power-Based PLL for Single-Phase Grid-Connected Power Conditioning Systems*. IEEE Transactions on Power Electronics 27(8): 3639-3650 (2012).

[15] Rodríguez F.J., Bueno E., Aredes M. et al., *Discrete-time Implementation of Second Order Generalized integrators for grid converters.* IEEE Industrial Electronics 10-13 Nov., pp. 176-181 (2008).

[16] Svensson J., *Synchronisation methods for grid-connected voltage source converters.* IEEE Generation, Transmission and Distribution 148(3): 229-235 (2001).

[17] Coluccio L., Eisinberg A., Fedele G. et al., *Modulating functions method plus SOGI scheme for signal tracking.* IEEE Industrial Electronics. ISIE 2008, pp. 854-859 (2008).

[18] Texas Instruments, TMS320F28069, Piccolo Microcontrollers, SPRS698C – November 2010 – Revised May (2012).

[19] Texas Instruments, TMS320x2803x Piccolo Control Law Accelerator (CLA), Reference guide, SPRUGE6B May 2009 – Revised May (2010).